A One-step Approach for Centralized Overactuated Motion Control of a Prototype Reticle Stage

Tacx, Paul; Oomen, Tom

DOI
10.1016/j.ifacol.2022.11.202

Publication date
2022

Document Version
Final published version

Published in
IFAC-PapersOnline

Available online at www.sciencedirect.com

ScienceDirect

IFAC Papers Online CONFERENCE PAPER ARCHIVE

IFAC PapersOnLine 55-37 (2022) 308–313

A One-step Approach for Centralized Overactuated Motion Control of a Prototype Reticle Stage

Paul Tacx * **Tom Oomen** *,**

* *Department of Mechanical Engineering, Eindhoven University of Technology, Eindhoven, The Netherlands.*
** *Faculty of Mechanical, Maritime, and Materials Engineering, Delft University of Technology, Delft, The Netherlands.*

Abstract: Next-generation motion stages are envisaged to be lightweight to meet stringent demands regarding accuracy and throughput. The lightweight stage design implies flexible dynamical behavior, which is foreseen to be severely excited due to increasing acceleration forces. The aim of this paper is to exploit additional actuators and sensors to explicitly control the flexible dynamic behavior. A systematic weighting filter design procedure is introduced which is tailored to next-generation motion stages. The presented procedure naturally connects to existing robust control techniques. The procedure is applied to an experimental next-generation reticle stage confirming performance enhancement by exploiting additional actuators and sensors beyond traditional performance limitations.

Keywords: Mechatronic systems, Motion Control Systems, Identification for Control, Identification and control methods, Modeling.

1. INTRODUCTION

Stringent demands regarding accuracy and throughput in next-generation motion systems require flexible-dynamic behavior to be controlled explicitly (Oomen, 2018). An important application is the production of semi-conductors which requires nanometer positioning (Van de Wal et al., 2002). A wafer scanner is a device that etches a desired IC pattern into a photosensitive layer on a silicon disc, called a wafer. During exposure, the image of the desired IC patterns, which is contained in the reticle stage (Fig. 1), is projected through a lens on the photoresist. During this entire process, both the reticle and the wafer must extremely accurately track a predefined reference trajectory in six motion degrees of freedom (DOFs). Development in the lithographic industry requires next-generation motion stages to achieve high machine throughput which requires high accelerations in all DOFs. For this reason, next-generation motion stages are designed to be lightweight (Oomen et al., 2014). As a consequence of the lightweight stage design, flexible dynamic behavior predominantly occurs at lower frequencies which has important consequences for next-generation motion control.

The flexible dynamic behavior in next-generation motion systems introduces limits on the achievable motion performance (Balas and Doyle, 1994). On the one hand, flexible dynamic behavior leads to inherently multivariable systems since the flexible dynamic behavior is generally not aligned with the DOFs. On the other hand, next-generation motion systems are envisioned to be equipped with many actuators and sensors to actively control flexible dynamic behavior (Oomen et al., 2014; Makarovic et al., 2004). In sharp contrast, for traditional motion systems, the number of actuators and sensors equals the number of DOFs. These developments motivate a model-based robust control approach that explicitly controls flexible dynamic behavior.

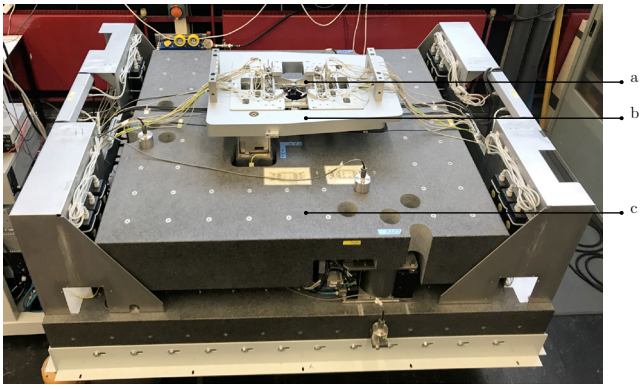

Fig. 1. Experimental reticle stage system, where (a) denotes the reticle stage, (b) the force frame, and (c) the active vibration isolation system.

Although several model-based robust control approaches have been presented and applied to deal with the inherently multivariable nature of next-generation motion stages, at present these techniques have not been tailored and applied to explicitly control the flexible-dynamic behavior of next-generation motion systems. In Ohnishi et al. (1996); Lee and Tomizuka (1996), robust control approaches are considered tailored towards motion con-

⋆ This work is part of the research programme VIDI with project number 15698, which is (partly) financed by the Netherlands Organisation for Scientific Research (NWO).

10.1016/j.ifacol.2022.11.202

trol. However, the approaches lack a connection with the system identification step which limits the attainable performance. A motion control design procedure is presented in Steinbuch and Norg (1998) that combines system identification and robust control for SISO motion systems. This approach is further refined towards multivariable systems in De Callafon and van den Hof (2001). However, in De Callafon and van den Hof (2001), the performance improvement is hampered by conservatism in the system identification procedure. In Oomen and Bosgra (2012); Oomen et al. (2014), an approach has been developed to explicitly deal with multivariable systems and is particularly suitable for next-generation motion stages. However, the approach in Oomen et al. (2014) is tailored to control the rigid-body DOFs. In Van Herpen et al. (2014), a methodology is proposed to explicitly control the flexible dynamic behavior. However, the flexible dynamic behavior is controlled using manual loop-shaping techniques which limits the achievable performance.

The main contribution of this paper is the application of a systematic one-step robust control design approach to go beyond the conventional performance limits through explicit control of the flexible dynamical behavior using additional actuators and sensors. Based on mechatronic insight, the weighting filters for robust control design are proposed. In contrast to Van Herpen et al. (2014), this paper offers a one-step approach for the robust control synthesis. The presented robust control design approach is applied to a next-generation prototype reticle stage system (Fig. 1), demonstrating the effectiveness of the approach proposed in this paper through comparison with the traditional control approach.

The paper is organized as follows. The setup and problem formulation are presented in Sec. 2. The theoretical aspects and a motivating example are presented in Sec. 3. An approach is proposed that exploits additional sensors and actuators to actively control the flexible dynamic behavior using robust control in Sec. 4. The proposed approach is applied in a case study in Sec. 5 on a next-generation reticle stage confirming a significant performance enhancement. This section is considered to be the main contribution of this paper. Conclusions are drawn in Sec. 6.

2. PROBLEM FORMULATION

2.1 Setup

The considered prototype floating reticle stage setup is depicted in Fig. 1. The aim of the reticle stage is to position the reticle with nanometer accuracy in 6 DOFs, i.e., 3 translations and 3 rotations. The reticle stage is actuated by 14 force actuators of which 8 actuators operate in the vertical direction. The actuators allow for contactless operations, hence, the system can operate under vacuum conditions. The system is equipped with an active vibration isolation system that isolates the metrology frame from environmental disturbances. The metrology frame contains 14 sensors that measure the position of the reticle stage with nanometer accuracy. The vertical positions are measured with 8 capacitive sensors, see Fig. 2. For motion control, the vertical directions are the most challenging due to the limited out-of-plane

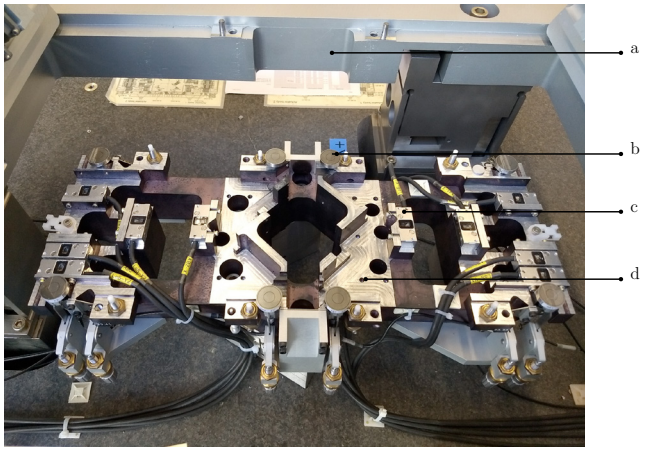

Fig. 2. Close up of the experimental reticle stage system, where (a) denotes the force frame, (b) denotes a capacitive vertical position sensor, (c) a horizontal position sensor, and (d) the metrology frame.

stiffness of the reticle stage. For this reason, this section focuses on the vertical direction. It is emphasized that the approach presented in this paper is aimed to control next-generation motion systems, i.e. systems with a large number of inputs and outputs. To facilitate exposition, only the vertical direction and the first vertical flexible mode are considered.

2.2 Problem Formulation

Flexible dynamic behavior introduces performance limitations in motion systems. The motion performance in traditional control configurations is limited by the flexible dynamic behavior. The aim of this paper is to go beyond traditional rigid-body-based control by actively controlling the flexible dynamic behavior. Specifically, the deformations caused by the flexible dynamics are actively controlled by exploiting additional actuators and sensors of the prototype reticle stage. A one-step robust control approach is pursued that enables high-performance motion control of the prototype reticle stage.

3. THEORETICAL ASPECTS AND MOTIVATING EXAMPLE

The aim of this section is to introduce the concept of exploiting additional sensors and actuators to go beyond the limits of traditional control configurations.

3.1 Theoretical Aspects

The standard control configuration is depicted in Fig. 3 where the plant is denoted by P and the controller by C. The extended control configuration is depicted in Fig. 4. The extended plant P^{ext} is defined by extending the standard configuration with the additional inputs and outputs.

Definition 1. The extended plant is defined as

$$P_{\text{ext}} : \tilde{u} \mapsto \tilde{y} \tag{1}$$

where $\tilde{u}$ and $\tilde{y}$ are defined as

$$\tilde{u} = \begin{bmatrix} u \\ u_{\text{ext}} \end{bmatrix} \qquad \tilde{y} = \begin{bmatrix} y \\ y_{\text{ext}} \end{bmatrix}. \tag{2}$$

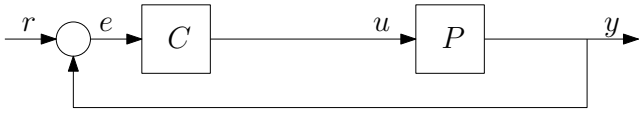

Fig. 3. Standard configuration.

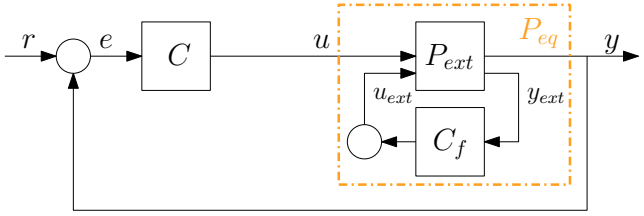

Fig. 4. Extended configuration.

Here, $u, y \in \mathbb{R}^n$ denote the n DOFs of the considered motion system and $u_{\text{ext}}, y_{\text{ext}}$ denote the additional inputs and outputs used to actively control the flexible modes.

Definition 2. The equivalent plant,see Fig. 4, is given by

$$P_{\text{eq}} = \mathcal{F}_l(P_{\text{ext}}, -C_f) \tag{3}$$
$$= P_{11} - P_{12}C_f(I + P_{22}C_f)^{-1}P_{21}. \tag{4}$$

3.2 Motivating Example

In this section, it is shown how additional sensors and actuators can be exploited to go beyond traditional rigid-body motion control by exploiting physical insight. To facilitate exposition, the simple two-mass-spring-damper system in Fig. 6 is considered. Consider the non-collocated transfer in Fig. 7. Observe that the flexible dynamic behavior at approximately 0.5 Hz does not introduce any right-half plane poles and zeros. However, from practical experience, it is known that the flexible dynamics limit the attainable performance unless the robustness criteria, e.g. phase margin, are loosened.

The additional actuator and sensor in Fig. 5 and 6 allow to go beyond the conventional limits on the attainable bandwidth. The position $x_{\text{diff}} = x_2 - x_1$ is measured and the force $F_{\text{diff}} = F_2 - F_1$ is actuated. This leads to the following extended plant definition

$$P_{\text{col,ext}} : \begin{bmatrix} F_1 \\ F_{\text{diff}} \end{bmatrix} \mapsto \begin{bmatrix} x_2 \\ x_{\text{diff}} \end{bmatrix}. \tag{5}$$

The additional actuator and sensor are exploited in the following two steps.

S1 A proportional controller is designed for the flexible mode $x_{\text{diff}} \mapsto F_{\text{diff}}$

$$C_f = k_c. \tag{6}$$

The aim of the feedback controller (6) is to actively control the flexible mode, e.g., by increasing the stiffness, the resonance is shifted to a higher frequency.

S2 The equivalent plant is determined by closing the feedback loop of the flexible mode, see Fig 4, enabling higher bandwidths.

From a mechatronics perspective, the flexible mode controller results in a higher stiffness which increases the resonance frequency. This is confirmed by the Bode plot of the equivalent plant in Fig 7. This concept is used in the following section to construct weighting filters for the robust control synthesis.

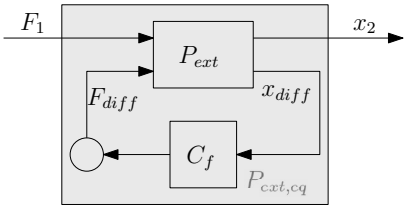

Fig. 5. Equivalent plant of the mechanical system in Fig. 6.

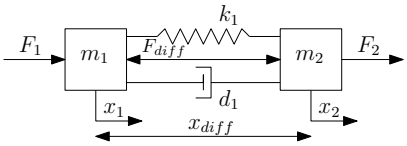

Fig. 6. The mechanical system considered in the motivational example.

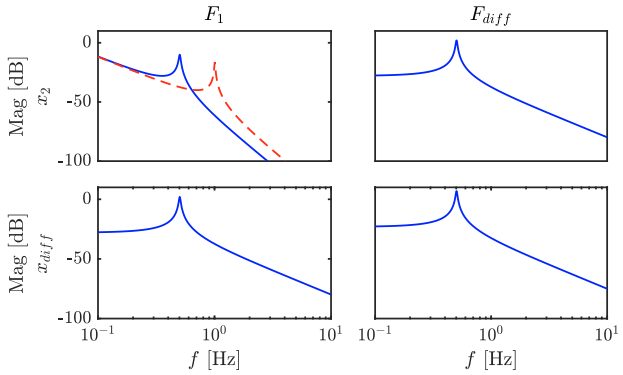

Fig. 7. Element-wise Bode magnitude plot of the extended plant (blue) and Bode magnitude of the equivalent plant (top left, red dashed).

4. APPROACH

In this section, the approach for exploiting additional actuators and sensors through explicit control of flexible dynamics in next-generation motion systems is introduced. First, the robust control setup is discussed. Thereafter, the weighting filter design strategy is discussed.

4.1 Robust Control Setup

A crucial aspect of the robust control approach is the control criterion.

Definition 3. The control goal is specified by the $\mathcal{H}_\infty$-norm-based control criterion

$$\mathcal{J}(P_{\text{ext}}, C) := \|WT(P_{\text{ext}}, C)V\|_\infty, \tag{7}$$

where $W = \text{diag}(W_y, W_u)$, $V = \text{diag}(V_2, V_1)$, and $W, V, W^{-1}, V^{-1} \in \mathcal{RH}_\infty$ are user-defined weighting filters.

The closed-loop feedback interconnection $T(P, C)$ is defined as

$$T(P_{\text{ext}}, C) = \begin{bmatrix} P_{\text{ext}} \\ I \end{bmatrix} (I + CP_{\text{ext}})^{-1} \begin{bmatrix} C & I \end{bmatrix}. \tag{8}$$

The criterion (7) in conjunction with the four-block interconnection facilitates the synthesis of internally stabilizing controllers (Skogestad and Postlethwaite, 2007). The criterion (7) is formulated such that it is to be minimized for the true system P_o, i.e., $C^{\text{opt}} = \arg\min_C \mathcal{J}(P_o, C)$.

The key idea in robust control is to consider a model set $\mathcal{P}$ such that

$$P_o \in \mathcal{P}. \tag{9}$$

Associated with the model set is the worst-case performance criterion

$$\mathcal{J}_{\mathrm{WC}}(\mathcal{P}, C) := \sup_{P \in \mathcal{P}} \mathcal{J}(P, C). \tag{10}$$

Consequently, by minimizing the worst-case performance criterion

$$C^{\mathrm{RP}} = \arg\min_{C}(\mathcal{P}, C) \tag{11}$$

it is guaranteed that

$$\mathcal{J}(P_o, C^{\mathrm{RP}}) \leq \mathcal{J}_{\mathrm{WC}}(\mathcal{P}, C^{\mathrm{RP}}). \tag{12}$$

The model set is constructed by considering a perturbation Δ around a nominal model $\hat{P}$

$$\mathcal{J} = \left\{ P \middle| P = \mathcal{F}_u(H, \Delta), \Delta \in \mathbf{\Delta} \right\}, \tag{13}$$

where the upper Linear Fractional Transformation (LFT) is given by

$$\mathcal{F}_u(\hat{H}, \Delta_u) = \hat{H}_{22} + \hat{H}_{21}\Delta \left(I - \hat{H}_{11}\Delta_u \right)^{-1} \hat{H}_{12}. \tag{14}$$

The transfer matrix $\hat{H}$ is defined as

$$\hat{H} : \begin{bmatrix} p \\ w \end{bmatrix} \mapsto \begin{bmatrix} q \\ z \end{bmatrix} = \begin{bmatrix} \hat{H}_{11} & H_{12} \\ \hat{H}_{21} & H_{22} \end{bmatrix} \tag{15}$$

The transfer matrix $\hat{H}$ contains the nominal model $\hat{P}$ and determines the internal structure of the model set. The perturbation set is a norm-bounded subset of $\mathcal{H}_\infty$

$$\mathbf{\Delta} = \{ \Delta \in \mathcal{RH}_\infty | \|\Delta\|_\infty \leq \gamma \}. \tag{16}$$

The parameter γ defines the $\mathcal{H}_\infty$-norm bound. The uncertainty set can be subject to additional constraints, such as parameter uncertainty from a polytope (Dullerud and Paganini, 2013), (Megretski and Rantzer, 1997). Throughout, unstructured uncertainty perturbations are considered to improve the readability of the results.

4.2 Weighting Filter Design

In this section, a systematic weighting filter design approach for multivariable robust control design is proposed to go beyond traditional limits by exploiting additional sensors and actuators. A loop-shaping-based weighting function design approach is pursued based on the approach in McFarlane and Glover (1992) and Vinnicombe (2001). The key benefit of the loop-shaping approach is that it can be effectively used to specify the open-loop requirements for motion systems, as shown in several motion control applications (Schonhoff and Nordmann, 2002), (Oomen and van der Meulen, 2013).

The weighting filters W and V are internally structured as

$$W = \begin{bmatrix} W_2 & 0 \\ 0 & W_1^{-1} \end{bmatrix} \qquad V = \begin{bmatrix} W_2^{-1} & 0 \\ 0 & W_1 \end{bmatrix}. \tag{17}$$

The weighting filters W_1 and W_2 are designed such that

$$P_{\mathrm{ext,s}} = W_2 P_{\mathrm{ext}} W_1 \tag{18}$$

has a certain desired open-loop shape. Subsequently, the robust control design incorporates the desired loop shape in the controller synthesis step, i.e. (11). Essentially the design of weighting filters for the extended plant (1) consists of two parts.

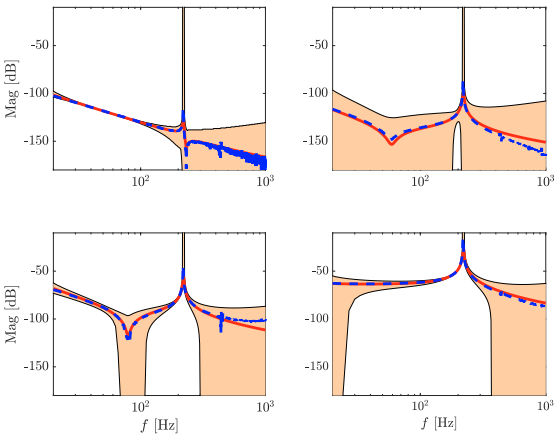

Fig. 8. Element-wise Bode Magnitude plot of the true system P_o (blue), nominal model $\hat{P}$ (red dashed), and model set $\mathcal{P}^{\mathrm{RCR}}$ (orange surface).

P1 First, consider the flexible behavior $P_{\mathrm{flex}} : u_{\mathrm{ext}} \mapsto y_{\mathrm{ext}}$. The weighting filters $W_{2,f}$ and $W_{1,f}$ should be shaped such that

$$P_{\mathrm{flex,s}} = W_{2,f} P_{\mathrm{flex}} W_{1,f} \tag{19}$$

resembles the desired behavior. Typically, a high gain is required for the flexible loop to increase the stiffness which results in an increased eigenfrequency.

P2 Second, the weighting filters for the motion DOFs $P_{\mathrm{rb}} = u \mapsto y$ are designed based on the equivalent plant

$$P_{\mathrm{eq}} = \mathcal{F}_l(P_{\mathrm{ext}}, -W_{2,f} W_{1,f}). \tag{20}$$

The equivalent plant resembles the motion DOFs the under control of the flexible loop. The shaped motion DOFs

$$P_{\mathrm{eq,s}} = W_{2,\mathrm{rb}} P_{\mathrm{eq}} W_{1,\mathrm{rb}} \tag{21}$$

are designed by the weighting filters $W_{2,\mathrm{rb}}$ and $W_{1,\mathrm{rb}}$ such that the desired motion DOFs behavior is described.

After the weighting filters have been designed, the weighting filters are combined

$$W_1 = \mathrm{diag}(W_{1,\mathrm{rb}}, W_{1,f}) \quad W_2 = \mathrm{diag}(W_{2,\mathrm{rb}}, W_{2,f}). \tag{22}$$

In Sec 5, the proposed weighting filter design framework is applied to an experimental next-generation reticle stage, and an overview of considerations is provided.

5. CASE STUDY

In this section, a robust control approach is considered to go beyond traditional bandwidth limitations by exploiting additional sensors and actuators. The approach is applied to an experimental next-generation reticle stage, see Fig. 1. The weighting filter design introduced in Sec. 4.2 is further refined and considerations are provided. The case study encompasses all steps from frequency response function identification to robust controller synthesis. In the last subsection, the new approach is compared to the traditional control configuration. This section is considered to be the main contribution of this paper.

5.1 Exploiting additional sensors and actuators

The aim of this subsection is to exploit additional sensors and actuators of the reticle stage using the method proposed in this paper. In this case study, the robust-control-relevant system identification procedure in Oomen et al. (2014) is considered since this approach enables high-performance motion controllers. The first step encompasses non-parametric system identification of the extended plant. Based on the frequency response function, the weighting filters are designed in the second step. The third step encompasses nominal parametric modeling using the non-parametric estimate and the weighting filters. The fourth step is to construct a non-conservative model set based on the nominal model such that (9) is satisfied. The fifth step is the robust controller synthesis. Each of the five steps is discussed in the following paragraphs.

Step 0: Non-parametric System Identification The measured non-parametric true system estimate is depicted in Fig. 8. The rigid-body and the first flexible mode are considered

$$P_o : \begin{bmatrix} F_{\text{rb}} \\ F_{\text{flex}} \end{bmatrix} \mapsto \begin{bmatrix} x_{\text{rb}} \\ x_{\text{flex}} \end{bmatrix} \tag{23}$$

which are obtained through modal decoupling. The motion DOF, $F_{\text{rb}} \mapsto x_{\text{rb}}$, clearly exhibits rigid-body behavior in the low-frequency range. At $f_{\text{res}} = 200$ Hz, a lightly-damped resonance occurs which corresponds to the first flexible mode. The achievable bandwidth is limited due to the occurrence of the flexible mode by standard control configurations, i.e. rigid-body control.

Step 1: Weighting Filter Design In this step, the weighting filters are designed according to the procedure introduced in Sec. 4.2. The procedure involves two steps. The first step considers the design of the desired loop shape of the flexible loop. The second step involves the design of the weighting filters for the motion DOF. In particular, the design aims to achieve a bandwidth of $f_{\text{BW}} = 180$ Hz in the motion DOF.

P1 In the first step, the additional control loop, i.e. the flexible loop, is exploited to enhance the performance of the motion DOF loop. To enable a bandwidth of 180 Hz in the motion DOF, it is essential to control the flexible loop with a high gain. A high gain is desired since this resembles an increased stiffness which counteracts the deformation of the reticle stage. However, in the low range, a low gain is desired to prevent static deformations of the reticle. For this reason, $W_{f,2}$ is equipped with a high-pass filter with a cutoff frequency of $f_{\text{res}}/5 = 40$ Hz. Similarly, at high frequencies, a low gain is desired to prevent the amplification of disturbances. Therefore, $W_{f,1}$ is equipped with a low-pass filter with a cutoff frequency of $f_{\text{res}} \cdot 3 = 600$ Hz. The gain of the weighting filters at $f_{\text{res}} = 200$ Hz is equally distributed between the weighting filters $W_{f,1}$ and $W_{f,2}$. The weighting filter design for the flexible loop is depicted in Fig. 9.

P2 In the second design step, the equivalent plant (20) is computed which resembles the motion DOF under the control of the flexible loop. Due to the high gain controller in the flexible loop, the flexible dynamic behavior is counteracted which enables design freedom for bandwidth enhancement in the motion DOF. The weighting filters of the motion DOF are based on common loop shaping goals for motion systems, e.g. (Oomen et al., 2014). The Bode plots of the weighting filters are depicted in Fig. 9. The weighting filters aim for the target bandwidth $f_{\text{BW}} = 180$ Hz, incorporate integrator action till $f_{\text{BW}}/3 = 60$ Hz, and incorporate roll-off with a cutoff of $f_{\text{BW}} \cdot 3 = 540$ Hz.

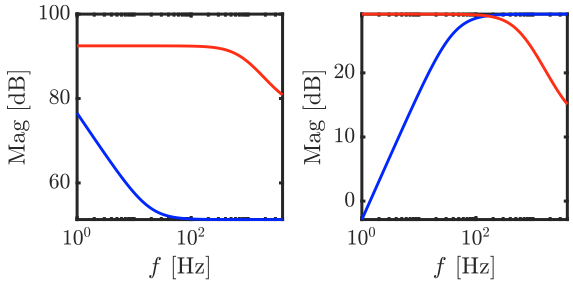

Fig. 9. Bode magnitude plots of the weighting filters of the motion DOF (left) $W_{1,\text{rb}}$ (blue) and $W_{2,\text{rb}}$ (red), and flexible loop (right) $W_{1,f}$ (blue) and $W_{2,f}$ (red).

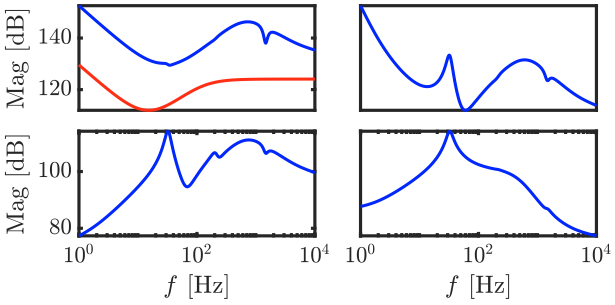

Fig. 10. Bode magnitude of the traditional manually tuned PID controller (red), and element-wise Bode plot of the robust controller C_{RP} (blue).

Step 2 & 3: Nominal Modeling and Model Set This step involves the nominal modeling step. This step is performed based on the robust-control-relevant system identification procedure in Oomen et al. (2014). The size of the $\mathcal{H}_\infty$-norm perturbation in (16) is computed by the procedure in Tacx and Oomen (2021). The resulting nominal model and model set are depicted in Fig. 8. The Bode plot reveals that the model set is tight for frequencies in the vicinity of the target bandwidth. Moreover, the flexible mode at $f_{\text{res}} = 200$ Hz is accurately modeled. However, at low frequencies, the model set is large and hence uncertain. A similar observation holds at higher frequencies. This specific behavior is attributed to the control-relevant coprime factors, see Oomen et al. (2014) for a detailed overview.

Step 4: Robust Control The fourth step involves the synthesis of the robust controller. The robust controller is synthesized based on the model set in Fig. 8 and the weighting filters in Fig. 9. The resulting element-wise Bode plot of the robust controller is depicted in Fig. 10.

5.2 Performance comparison

When designing a manually tuned PID controller for the standard motion control approaches, i.e. based on the

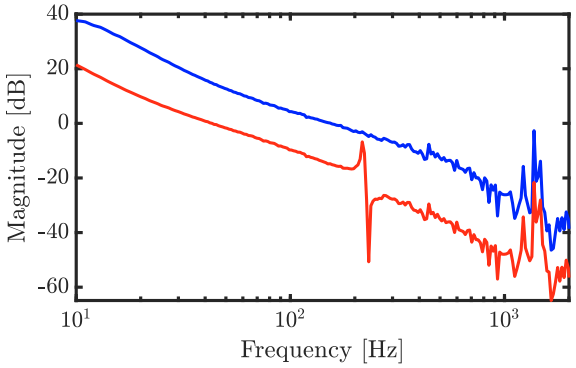

Fig. 11. Bode magnitude of the open-loop under the control of the traditional manually tuned PID rigid-body controller (red) and the equivalent motion DOF under the control of the robust controller C_{RP} (blue).

rigid-body configuration without the use of the additional flexible loop, the bandwidth is limited to approximately 50 Hz while maintaining decent robustness margins. Such a motion controller and open-loop are depicted in Fig. 10 and 11. Alternatively, notch filters can be used to counteract the flexible dynamics. However, this method does not extend to full MIMO systems due to inherent coupling in next-generation motion systems.

In sharp contrast, the method introduced in this paper allows going beyond the performance limitations encountered in traditional control configurations. In particular, the equivalent motion DOF plant under control of the flexible loop depicted in Fig. 11, i.e. the equivalent open-loop $\mathcal{F}_l(P_{\text{ext}}C^{RP}, -1)$, reveals that the robust controller achieves a bandwidth of 160 Hz which confirms a significant performance enhancement.

6. CONCLUSIONS

The motion performance of next-generation motion stages is limited by flexible dynamic behavior. In this paper, a systematic approach is introduced to explicitly control the flexible dynamic behavior by exploiting additional actuators and sensors. A robust control-based approach is pursued and a weighting filter design method is introduced. The proposed method is successfully applied to a next-generation reticle stage enabling significant performance enhancements compared to the traditional control configuration.

ACKNOWLEDGEMENTS

The authors wish to thank Raaf Bartelds for performing the experiments, the assistance in the robust control analysis, and the fruitful discussions.

REFERENCES

Balas, G.J. and Doyle, J.C. (1994). Control of lightly damped, flexible modes in the controller crossover region. *Journal of Guidance, Control, and Dynamics*, 17(2), 370–377.

de Callafon, R.A. and van den Hof, P.M. (2001). Multivariable feedback relevant system identification of a wafer stepper system. *IEEE Transactions on Control Systems Technology*, 9(2), 381–390.

Dullerud, G.E. and Paganini, F. (2013). *A course in robust control theory: a convex approach*, volume 36. Springer Science & Business Media.

Lee, H.S. and Tomizuka, M. (1996). Robust motion controller design for high-accuracy positioning systems. *IEEE Transactions on Industrial Electronics*, 43(1), 48–55.

Makarovic, J., Schneiders, M., van der Wielen, A., Lomonova, E., van de Molengraft, M., van Druten, R., Compter, J., Steinbuch, M., and Schellekens, P. (2004). Integrated design of a lightweight positioning system. In *7th International Conference on Motion and Vibration Control*. Citeseer.

McFarlane, D. and Glover, K. (1992). A loop-shaping design procedure using h_∞ synthesis. *IEEE transactions on automatic control*, 37(6), 759–769.

Megretski, A. and Rantzer, A. (1997). System analysis via integral quadratic constraints. *IEEE Transactions on Automatic Control*, 42(6), 819–830.

Ohnishi, K., Shibata, M., and Murakami, T. (1996). Motion control for advanced mechatronics. *IEEE/ASME transactions on mechatronics*, 1(1), 56–67.

Oomen, T. (2018). Advanced motion control for precision mechatronics: Control, identification, and learning of complex systems. *IEEJ Journal of Industry Applications*, 7(2), 127–140.

Oomen, T. and Bosgra, O. (2012). System identification for achieving robust performance. *Automatica*, 48(9), 1975–1987.

Oomen, T. and van der Meulen, S. (2013). High performance continuously variable transmission control through robust control-relevant model validation. *Journal of Dynamic Systems, Measurement, and Control*, 135(6).

Oomen, T., van Herpen, R., Quist, S., van de Wal, M., Bosgra, O., and Steinbuch, M. (2014). Connecting system identification and robust control for next-generation motion control of a wafer stage. *IEEE Transactions on Control Systems Technology*, 22(1), 102–118.

Schonhoff, U. and Nordmann, R. (2002). A $\mathcal{H}_\infty$-weighting scheme for PID-like motion control. In *Proceedings of the International Conference on Control Applications*, volume 1, 192–197. IEEE.

Skogestad, S. and Postlethwaite, I. (2007). *Multivariable feedback control: analysis and design*, volume 2. Citeseer.

Steinbuch, M. and Norg, M.L. (1998). Advanced motion control: An industrial perspective. *European Journal of Control*, 4(4), 278–293.

Tacx, P. and Oomen, T. (2021). Accurate $\mathcal{H}_\infty$-norm estimation via finite-frequency norms of local parametric models. In *2021 American Control Conference (ACC)*, 332–337. IEEE.

van de Wal, M., van Baars, G., Sperling, F., and Bosgra, O. (2002). Multivariable $\mathcal{H}_\infty/\mu$ feedback control design for high-precision wafer stage motion. *Control engineering practice*, 10(7), 739–755.

van Herpen, R., Oomen, T., Kikken, E., van de Wal, M., Aangenent, W., and Steinbuch, M. (2014). Exploiting additional actuators and sensors for nano-positioning robust motion control. *Mechatronics*, 24(6), 619–631.

Vinnicombe, G. (2001). Uncertainty and feedback $\mathcal{H}_\infty$ loop-shaping and the ν-gap metric.